Strong deviations from jellium behavior in the valence electron dynamics of potassium

Simo Huotari,[1] Christian Sternemann,[2] M. Claudia Troparevsky,[3,4] Adolfo G. Eguiluz,[3,4] Martin Volmer,[2] Henning Sternemann,[2] Harald Müller,[1] Giulio Monaco,[1] and Winfried Schülke[2]

[1]*European Synchrotron Radiation Facility, Boîte Postale 220, F-38043 Grenoble Cedex 9, France*

[2]*Fakultät Physik/DELTA, Technische Universität Dortmund, D-44221 Dortmund, Germany*

[3]*Department of Physics & Astronomy, University of Tennessee, Knoxville, Tennessee 37996, USA*

[4]*Materials Science & Technology Division, Oak Ridge National Laboratory, Oak Ridge, Tennessee 37831, USA*

(Received 6 July 2009; revised manuscript received 1 September 2009; published 2 October 2009)

We present experimental and *ab initio* theoretical determination of the dynamics of valence electrons in potassium by investigating the dynamical structure factor at nonvanishing momentum transfers. The spectra show large deviations from a jellium-type behavior due to the presence of *d*-type states above the Fermi level. In particular, we identify two well-defined interband excitations that have a direct correspondence with the density of states above the Fermi level.

DOI: 10.1103/PhysRevB.80.155107 PACS number(s): 78.70.Ck, 71.10.Ca, 71.45.Gm

I. INTRODUCTION

The valence electrons in alkali metals are typically considered as nature's closest realization of a free-electron gas (jellium). This is manifested, e.g., in their Fermi surfaces, which are nearly spherical. The fundamental electronic excitation in jellium is the plasmon, a collective charge-density excitation that can be studied using electron-energy-loss spectroscopy (EELS) (Refs. 1 and 2) and inelastic x-ray scattering (IXS) spectroscopy.[3] Within the so-called random-phase approximation (RPA), the energy of the plasmon is predicted to follow a dispersion $E_{pl}(q)=E_{pl}(0)+\alpha q^2$, where q is the exchanged momentum ($\hbar=1$), $\alpha=(3E_F)/[5E_{pl}(0)]$ is the dispersion constant, and E_F is the Fermi energy (2.0 eV for K). Measurements of the plasmon dispersion in alkali metals Rb and Cs showed important deviations from the RPA-predicted behavior,[4] implying $\alpha\approx 0$ for Rb and even $\alpha<0$ for Cs. A debate on the origin of the disagreement[4–6] has led to the conclusion that both band-structure and correlation effects modify the electron dynamics strongly in the case of heavy alkali metals.

Beyond simply studying the plasmon dispersion, the investigation of the *fine structure* of its lineshape revealed double-plasmon (pl-pl) excitations[7,8] in metals whose dynamical response is free-electron-like (e.g., Na, Al, and Mg). The experimentally observed pl-pl excitations are believed to be solely correlation-induced.[9,10] The present study originated from an attempt to determine the pl-pl excitations probability in K, but as a surprise we found that the many-body pl-pl excitations were hidden by the much stronger response of the empty *d* bands. Thus here we emphasize the message that the textbook view of the electronic degrees of freedom of the alkali metals beyond Na is oversimplified even in ambient conditions, by showing that even K displays strong non-jellium-type behavior when its electron dynamics is studied beyond the small momentum-transfer limit.

The most important reason for non-jellium-type behavior of the alkali metals is the empty conduction band with *d* symmetry, which approaches the Fermi level as the alkali-metal atomic number Z increases.[5] The density of states (DOS) of K valence electrons is nearly free-electron-like up to the Fermi energy, but the empty states have strong deviations from the free-electron model due to the *d* bands, which lie at energies comparable with the natural energy for electronic excitations in K—the ~4 eV plasmon energy. It was, for instance, shown that these empty *d* states are indirectly responsible for the anomalous plasmon lifetime dispersion in K.[11,12] However, up to now experimental data have been restricted to low-momentum transfers,[4] limiting the interband transitions by the dipole selection rule. It is well-known[13,14] that when the interaction of the electron with the probe involves a finite momentum transfer, higher-order excitations (e.g., $s\rightarrow d$) become allowed, and in this way the empty non-jellium *d*-symmetry states of the K valence electrons should turn directly visible in the electron response function.

When momentum transfer is increased, EELS starts to suffer from multiple-scattering events, which eventually dominate the spectra. IXS does not suffer from this limitation, and it represents a valuable complementary probe at large momentum transfers. The difference between IXS and EELS arises mostly from a much larger scattering probability in EELS. This has made EELS experiments often easier, and has for a long time limited IXS to the study of low-Z systems, where the large probing depth compensates the low cross section. However, third-generation synchrotron radiation sources and the recent developments of instrumentation[15–20] have rendered IXS a standard tool in studies of dielectric response. The advantages include true bulk sensitivity (in the millimeter range), an access to an almost unlimited range of exchanged wave vectors, and the possibility to study samples in gaseous or liquid phases,[21–24] or in extreme environments. While the alkali-metal studies by EELS concentrated on the plasmon dispersion and lifetime in the small-q limit, it has turned out that these observables alone are not necessarily sufficient for understanding the dynamical response of the electrons; for example, the *fine structure* of the plasmon-excitation lineshape contains new information on the effects of the band structure and correlation on the dynamical screening. In the momentum-transfer region $q\gtrsim q_c$, where q_c is the critical plasmon cutoff momentum, several IXS studies revealed behavior of the dynamical structure factor that could not be explained within the RPA-based free-electron model, namely a double-peak structure,[24–27]

and a high-energy shoulder.[7,8] These features are typical for real metals and semiconductors, where band-structure effects, and to a lesser extent correlation effects have to be considered. It has been shown that the double-peak structure is caused by band-structure effects and is an intrinsic property of noninteracting electrons[28] but correlation is not to be underestimated either, as can be seen from a better agreement between certain experiments and calculations based on a higher level of correlation as compared to the RPA.[7,8,10,29–31]

In this paper, we present a combined experimental and theoretical study of the dynamical response of valence electrons of K for finite wave vectors using IXS. We show that the response exhibits strong deviations from the jellium behavior. In the process, we demonstrate that an inspection of the *ab initio* response function, coupled with the IXS data, gives direct information on excited states of K.

II. THEORY

Our calculations are based on the evaluation of the dynamical density response function $\chi(\mathbf{r},\mathbf{r}',\omega)$ within time-dependent density-functional theory (TDDFT).[32] In TDDFT, χ obeys the formally exact integral equation[33–35] $\chi=\chi^s+\chi^s(v+f_{xc})\chi$, where χ^s is the density response function for Kohn-Sham electrons, v is the Coulomb interaction, and f_{xc} is the many-body kernel. χ^s was calculated for a ground state obtained in the local-density approximation (LDA), using the linearized augmented plane-wave (LAPW) method.[36] The crystal-local-field effects, i.e., the matrix nature of χ^s in reciprocal space, were fully taken into account; it turns out that a matrix of rank 13 suffices. As for the many-body kernel, we use the popular "adiabatic extension" of LDA, which defines the so-called TDLDA approximation for the physical response function χ.[34]

The connection between theory and experiment is given by the dynamical structure factor[3] $S(\mathbf{q},\omega)=-2V\,\mathrm{Im}\,\chi_{\mathbf{G_q},\mathbf{G_q}}(\mathbf{q}-\mathbf{G_q},\omega)$, where $\mathbf{G_q}$ is the unique $\mathbf{G}$ vector which brings $\mathbf{q}$, i.e., the momentum transfer into the first Brillouin zone, and V is the system volume. The calculations were done for $\mathbf{q}$ along the [100], [110], and [111] directions. Polycrystalline spectra were estimated by taking the multiplicity-weighted average of the three directional spectra in order to compare with the experiment. This is emphasized from hereon by considering the measurable functions as a function of $q=|\mathbf{q}|$ only. The calculations used a constant lifetime broadening of 0.2 eV.

Figure 1 shows the calculated density of states of bcc K. In the LAPW method, the DOS includes contributions from nonoverlapping "atomic spheres" (whose radii are typically ~2 a.u.) and from the interstitials between the atomic spheres. For our discussion, the main point to note is that inside the atomic spheres the DOS is decomposed into contributions from states labeled by their angular momentum content, and that above the Fermi level, the $l=2$ states dominate the DOS. In fact, the total DOS is easily visualized to be dominated by the sharp spikes due to the d states for energies on the order of the 4 eV plasmon energy (below the Fermi level the total DOS is controlled by the interstitials, which is dominated by delocalized, free-electron-like states). These states have strongly non-free-electron-like DOS. Most noteworthy are dips due to an absence of states at 6 and 9 eV above the Fermi level. The interstitial DOS is not decomposed into different symmetries here, but they do consist of mostly s-type states up to the Fermi energy, after which the spiky structures are created by d states in an analogy to the DOS of the atomic spheres. In general, the DOS above the Fermi surface is dominated by states primarily of d character. Now the d-type empty states are not reached from the occupied s states with small momentum transfers because $s\rightarrow d$ transitions are dipole forbidden. It is possible, however, to observe these quadrupolar transitions if the momentum transfer is increased.[13,14]

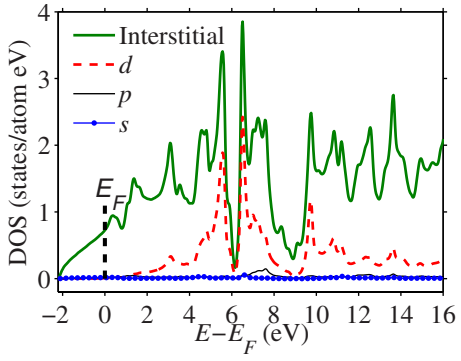

FIG. 1. (Color online) The DOS of bcc K, as calculated within LDA, using the LAPW method (Ref. 36). Contributions from the atomic spheres and the interstitials are shown; the former is decomposed into contributions from states of s, p, and d symmetries.

III. EXPERIMENT

The measurements of $S(q,\omega)$ were performed at the beamline ID16 of the European Synchrotron Radiation Facility with 9.9 keV radiation.[15] The incident beam was monochromatized by a combination of a double-crystal Si(111) premonochromator and a Si(220) channel cut to a bandwidth of 0.5 eV. The spectrometer was a Rowland-circle-based Johann-type crystal spectrometer operating in a near-backscattering geometry using a spherically bent Si(555) analyzer crystal with a bending radius of 1 m. The total energy resolution was 0.7 eV (Gaussian full-width-at-half-maximum). The sample was an approximately 100 μm thick K foil prepared inside an Ar-filled glove box on a steel holder. On the beamline, the holder was evacuated to a vacuum better than 10^{-6} mbar for the measurements. The sample was polycrystalline to a good approximation. A typical intensity was 100–200 counts/s in the plasmon peak and a background of about 1 count/s as measured on the negative-energy-loss side of the quasielastic line. The measurements of the $S(q,\omega)$ were performed in the energy-transfer range $\omega=0-22$ eV and momentum-transfer range $q=2.9-14.2$ nm^{-1}. The critical cutoff momentum for plasmons in K within the RPA is 7.4 nm^{-1}.

All spectra were measured several times and after a normalization to the incident photon flux the individual spectra

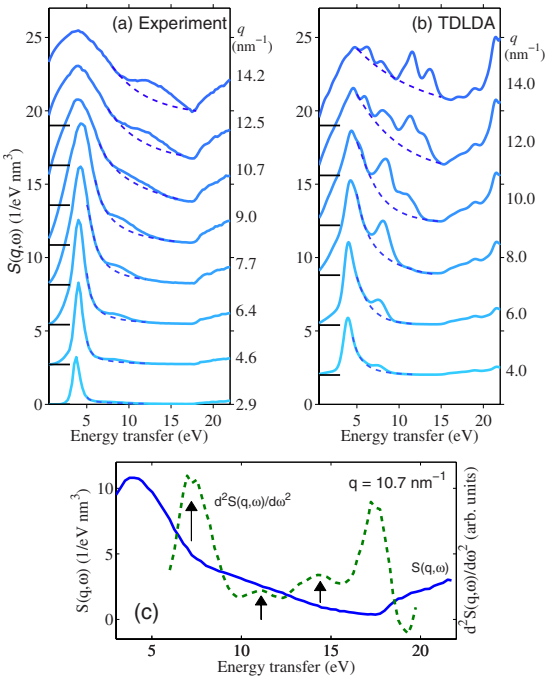

FIG. 2. (Color online) (a) Experimental and (b) TDLDA-based theoretical $S(q,\omega)$ of K for a range of momentum transfers. The individual spectra have been shifted on the vertical scale for clarity. The momentum-transfer values are marked on the right of each curve. The rise in the spectral weight beyond 18 eV is due to the excitation of K $M_{2,3}$ core electrons. A fit to remove the main excitation spectrum is shown as a dashed line in all cases. (c) The determination of the peaks of the cubic-spline-smoothed second derivative of $S(q,\omega)$ with respect to energy transfer for $q=10.7$ nm^{-1}. The positions of the peaks are marked with arrows.

were found to be identical. This confirms a negligible degradation of the sample. The sample was also monitored visually during the experiment and no reactions were observed. The quasielastic line tail was subtracted by fitting the low-ω limit of $S(q,\omega)$ with a quadratic function with the constraint $S(q,0)=0$. This yields reliable spectra for energy transfers above 3 eV. Due to the close presence of the K $M_{2,3}$ edges at 18 eV, an absolute normalization of the experimental spectra is difficult. Thus they were normalized to the same area as the theoretical ones up to energy transfers of 18 eV. While the procedure does not necessarily give reliable absolute cross sections, it does not affect the spectral shape for each individual $S(q,\omega)$.

IV. RESULTS AND DISCUSSION

Figures 2(a) and 2(b) show the $S(q,\omega)$ for polycrystalline K measured and calculated as described above. The theoretical spectra as shown here were convoluted with the experimental resolution function. The energy-loss structure is dominated by a peak at around 4 eV, which corresponds to the plasmon excitation for $q<q_c$, transforming to a particle-hole band for $q>q_c$. With an increasing momentum transfer, this excitation spectrum disperses to energies slightly higher than 4 eV and broadens. Most interestingly, a high-energy feature starts to develop at 8 eV. This is in agreement with an earlier theoretical study, predicting a similar feature[5] and possibly related to a structure seen in optical reflectance and absorption measurements.[37] The feature seems at first sight to disperse toward higher energies up to 13 eV at the highest measured momentum transfer. The calculated spectra agree well with the experimental result at low momentum transfers, but at higher momentum transfers it is clear that *two* separate and very pronounced features develop, one at 8 eV (well-defined for $q<12$ nm^{-1}) and another at 11 eV (well-defined for $q>10$ nm^{-1}). Despite the fact that the theory seems to predict sharper and more intense features than are seen in the experiment, the qualitative behavior seems to set out correctly; the main differences are in the width and the intensity of the related features. We assign these structures to be due to the fine structure of the DOS as seen in Fig. 1. In particular, the unoccupied DOS exhibits two pronounced gaps that are also visible in the spectra as excitation gaps. Similar excitation gaps have also been found in other metals.[38,39] To identify the spectral features, we have used two different ways to extract their dispersion from the theoretical and the experimental data. First we have isolated the maxima of the second derivatives of the dynamical structure factor with respect to the energy transfer, i.e., of $d^2S(q,\omega)/d\omega^2$. We used a cubic-spline smoothing of the experimental data to compute the second derivative. The energies of these maxima that correspond to dips in the spectra reveal the positions of the excitation gaps. One example of such determination is shown in Fig. 2(c). The second method aims at the isolation of the resulting peaklike structures of the excitation spectrum in order to better visualize the comparison between experiment and theory. This was done by fitting a sum of a Pearson VII function plus a constant to mimic the main excitation spectrum tail before the onset of the high-energy features, in a similar fashion as has been described in Refs. 7 and 8. Exactly the same procedure was applied to the experimental and to the theoretical data, and the resulting fits are shown as dashed lines in Fig. 2. The results of the extraction procedures are shown in Fig. 3, which depicts the relevant q, ω region after the subtraction of the fit. The dispersion of the excitation-gap-induced dips of the spectra is shown in the same figure.

The qualitative behavior of the experimental and theoretical results is in agreement, and the striking result is that an existence of two or three separate peaks is confirmed for experiment and theory, respectively. One, labeled A, is a slightly dispersing peak around 8–9 eV, appearing at around 5 nm^{-1} and disappearing after 11 nm^{-1} (experiment) or 13 nm^{-1} (theory). A second feature, labeled B, which in the theoretical result is as strong as the first one but in experiment about twice as strong as compared to the feature A, starts to build up spectral weight after 11 nm^{-1} and is found at around 12 eV (theory) or 13 eV (experiment). The feature C can be distinguished from the feature B only in the theoretical result, while in the experiment it is merged with the peak B. In general, it seems that the excitations have about 1 eV higher energies as revealed by the experiment than they appear in the theoretical prediction, which could be due to effects beyond the TDLDA. Investigations for even higher momentum transfers would be interesting to observe the full dispersion of the feature B+C.

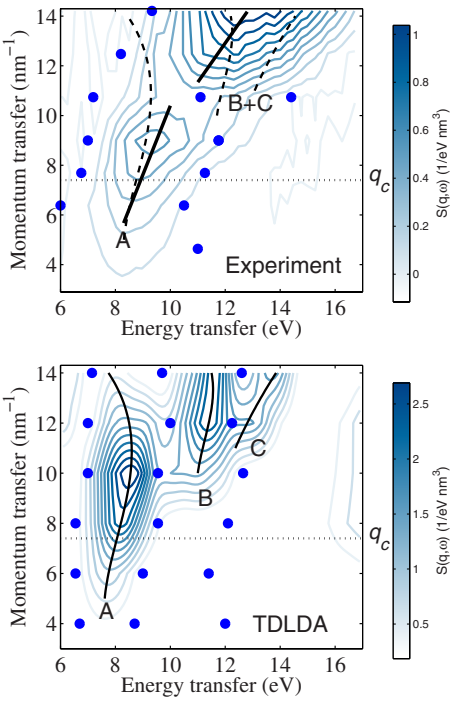

FIG. 3. (Color online) Extracted high-energy features obtained by subtracting the fitted main excitation spectrum from the band-structure-related features, for both experiment and theory within TDLDA. The observable excitations are labeled A-C and their dispersion is shown with solid lines that act as guides to the eyes. The filled circles show the dispersion of the excitation gaps, deducted via second derivatives of the dynamical structure factor as described in the text. Dashed lines overlaid with the experimental data show the dispersion of the theoretical peaks A-C shifted by 0.7 eV for comparison.

The interpretation of the observed excitation-gap—excitation-peak structures lies on the band-structure picture and the sharp features in the empty DOS of Fig. 1 which we identify next. The absence of electron states at certain energies leads inevitably to excitation gaps, manifesting themselves as dips in the spectra. We assign the spectral features directly to the shape of the DOS as seen in Fig. 1. The dip at 6–7 eV originates from the gap in the DOS at 6 eV, and the dip at 9 eV originates from the DOS gap at 9 eV. The remaining peaklike structure A at 8 eV originates from electrons transferred to the states at 6–8 eV above the Fermi level, between the two excitation gaps, and the excitation peaks B+C to states above the DOS gap at 9 eV. The fine structure, most notably the splitting of the structures B and C in the theory, reflects the fine structure of the DOS above 10 eV. The excitations B and C are indiscernible in the experimental spectra probably due to two reasons: either it is a manifestation of the underlying fine structure of the DOS above the second gap for energies above 10 eV, or energy-dependent lifetime broadening that could merge them together,[40] or a combination of the two. Interestingly, as the peaks B and C are merged together in the experiment, so are also the corresponding excitation gaps, resulting in one gap at 11 eV in experiment as opposed to two gaps at 9 and 12 eV in theory. It should be noted that the physical reasons for the structures are the excitation gaps. The separation of the resulting excitation peaks serves as an additional tool to compare experiment and theory—most importantly the fine structure of the DOS. Most noteworthy about the comparison made here is that (i) the response of the simple K metal is highly non-jellium-type when probed with finite momentum transfer, and (ii) very direct information of the empty DOS can be gained via the mere inspection of the measured loss function as the structures in the spectra are a direct consequence of the structure in the unoccupied DOS.

The observed peaklike structures A and B+C are completely distinct from the coherent collective double-plasmon excitations,[7–9] which have been observed in several simple metals. The latter excitations have a similar spectral range but expected to be much weaker. The results thus emphasize the overlap of band-structure-dependent fine structures of the $S(q,\omega)$ with correlation-induced ones showing the difficulties separating them in many systems, and that the dynamical response of the valence electrons of K deviates strongly from a jellium response—much more than that of Na or Mg for instance.[7,8] Similar excitation gaps have been found also in other metals[38,39] and in general such gaps seem to be often present in real metals—but in the present case of K they are surprisingly pronounced in the view of the alkali-metal nature of the material. There are also other mechanisms that can cause highly non-jellium-type behavior even in nearly free-electron metals. Typical examples are the so-called zone-boundary collective states[41–44] that originate from the removal of the degeneracy of states on Bragg planes. This may produce excitation gaps and consequently near-zero crossings of the real part of the dielectric functions, which in turn can give additional structures in the response function. These structures are highly anisotropic and would be completely washed out in polycrystalline materials as used in this investigation. So the very strong *d*-band-based structures seen here are traced back either to a crystal-field splitting or to an energy downshift in *d* states relative to their empty-lattice counterparts due to the lack of *d*-core states.[38]

V. CONCLUSIONS

We have shown here spectra of the dynamical structure factor for K for large momenta. When the detailed shape of the dynamical structure factor of K is studied for large momentum transfers ($q_c < q < 2q_c$), the plasmon decays and band-structure effects start to play an increasingly larger role. Strikingly, large nonjellium behavior dominates the spectra at momentum transfers on the order of $2q_c$. Even if the plain plasmon dispersion might follow the prediction of a free-electron-gas model, the detailed shape of the excitation spectrum reveals new information on the interplay of correlation and band-structure-related effects. Especially, the pronounced fine structure of the empty DOS is directly manifested in the energy-loss function. The enhancement of the corresponding *s*-*d* transitions is due to the increased nondipole contribution in the scattering cross section with increasing momentum transfer, accessible by inelastic x-ray scattering spectroscopy. In particular, we have identified excitation-

gap—excitation-peak fine structure both experimentally and theoretically between the energies of 8–13 eV.

While the agreement between the experiment and theory is good, the remaining discrepancies are probably due to exchange and correlation effects to be accounted for in an implementation of TDDFT beyond the TDLDA, and energy-dependent lifetime effects.

ACKNOWLEDGMENTS

A. G. E. acknowledges support from NSF ITR under Grant No. DMR-0219332. M. C. T. was partially supported by the DOE CMSN-PCSCS network. Computations were done at the National Energy Research Scientific Computing Center (NERSC). We are grateful to C. Henriquet for expert technical assistance, and M. Tolan for his support.

[1] J. Fink, Adv. Electron. Electron Phys. **75**, 121 (1989).
[2] F. J. García de Abajo, Rev. Mod. Phys. (to be published).
[3] W. Schülke, *Electron Dynamics by Inelastic X-Ray Scattering* (Oxford University Press, Oxford, 2007).
[4] A. vom Felde, J. Sprösser-Prou, and J. Fink, Phys. Rev. B **40**, 10181 (1989).
[5] F. Aryasetiawan and K. Karlsson, Phys. Rev. Lett. **73**, 1679 (1994).
[6] A. Fleszar, R. Stumpf, and A. G. Eguiluz, Phys. Rev. B **55**, 2068 (1997).
[7] C. Sternemann, S. Huotari, G. Vankó, M. Volmer, G. Monaco, A. Gusarov, H. Lustfeld, K. Sturm, and W. Schülke, Phys. Rev. Lett. **95**, 157401 (2005).
[8] S. Huotari, C. Sternemann, W. Schülke, K. Sturm, H. Lustfeld, H. Sternemann, M. Volmer, A. Gusarov, H. Müller, and G. Monaco, Phys. Rev. B **77**, 195125 (2008).
[9] K. Sturm and A. Gusarov, Phys. Rev. B **62**, 16474 (2000).
[10] H. M. Böhm, R. Holler, E. Krotscheck, and M. Panholzer, J. Phys. A **42**, 214036 (2009).
[11] K. Sturm, Solid State Commun. **25**, 797 (1978).
[12] W. Ku and A. G. Eguiluz, Phys. Rev. Lett. **82**, 2350 (1999).
[13] S. Doniach, P. M. Platzman, and J. T. Yue, Phys. Rev. B **4**, 3345 (1971).
[14] J. A. Soininen, A. Mattila, J. J. Rehr, S. Galambosi, and K. Hämäläinen, J. Phys.: Condens. Matter **18**, 7327 (2006).
[15] R. Verbeni, T. Pylkkänen, S. Huotari, L. Simonelli, G. Vankó, K. Martel, C. Henriquet, and G. Monaco, J. Synchrotron Radiat. **16**, 469 (2009).
[16] F. Gélebart, M. Morand, Q. Dermigny, P. Giura, J.-P. Rueff, and A. Shukla, AIP Conf. Proc. **879**, 1837 (2007).
[17] S. Huotari, G. Vankó, F. Albergamo, C. Ponchut, H. Graafsma, C. Henriquet, R. Verbeni, and G. Monaco, J. Synchrotron Radiat. **12**, 467 (2005).
[18] Y. Q. Cai, P. Chow, C. C. Chen, H. Ishii, K. L. Tsang, C. C. Kao, K. S. Liang, and C. T. Chen, AIP Conf. Proc. **705**, 340 (2004).
[19] J. P. Hill, D. S. Coburn, Y.-J. Kim, T. Gog, D. M. Casa, C. N. Kodituwakku, and H. Sinn, J. Synchrotron Radiat. **14**, 361 (2007).
[20] T. T. Fister, G. T. Seidler, L. Wharton, A. R. Battle, T. B. Ellis, J. O. Cross, A. T. Macrander, W. T. Elam, T. A. Tyson, and Q. Qian, Rev. Sci. Instrum. **77**, 063901 (2006).
[21] C. A. Burns, P. Abbamonte, E. D. Isaacs, and P. M. Platzman, Phys. Rev. Lett. **83**, 2390 (1999).
[22] C. A. Burns, P. Giura, A. Said, A. Shukla, G. Vankó, M. Tuel-Benckendorf, E. D. Isaacs, and P. M. Platzman, Phys. Rev. Lett. **89**, 236404 (2002).
[23] H. Hayashi, Y. Udagawa, C.-C. Kao, J.-P. Rueff, and F. Sette, J. Electron Spectrosc. Relat. Phenom. **120**, 113 (2001).
[24] J. P. Hill, C.-C. Kao, W. A. C. Caliebe, D. Gibbs, and J. B. Hastings, Phys. Rev. Lett. **77**, 3665 (1996).
[25] P. M. Platzman and P. Eisenberger, Phys. Rev. Lett. **33**, 152 (1974).
[26] P. M. Platzman, E. D. Isaacs, H. Williams, P. Zschack, and G. E. Ice, Phys. Rev. B **46**, 12943 (1992).
[27] W. Schülke, H. Nagasawa, and S. Mourikis, Phys. Rev. Lett. **52**, 2065 (1984).
[28] A. Fleszar, A. A. Quong, and A. G. Eguiluz, Phys. Rev. Lett. **74**, 590 (1995).
[29] H.-C. Weissker, J. Serrano, S. Huotari, F. Bruneval, F. Sottile, G. Monaco, M. Krisch, V. Olevano, and L. Reining, Phys. Rev. Lett. **97**, 237602 (2006).
[30] S. Galambosi, J. A. Soininen, K. Hämäläinen, E. L. Shirley, and C.-C. Kao, Phys. Rev. B **64**, 024102 (2001).
[31] I. G. Gurtubay, J. M. Pitarke, W. Ku, A. G. Eguiluz, B. C. Larson, J. Tischler, P. Zschack, and K. D. Finkelstein, Phys. Rev. B **72**, 125117 (2005).
[32] E. Runge and E. K. U. Gross, Phys. Rev. Lett. **52**, 997 (1984).
[33] M. Petersilka, U. J. Gossmann, and E. K. U. Gross, Phys. Rev. Lett. **76**, 1212 (1996).
[34] E. K. U. Gross, J. F. Dobson, and M. Petersilka, *Density Functional Theory II* (Springer, New York, 1996), p. 81.
[35] K. Burke and E. K. U. Gross, *Density Functionals: Theory and Applications* (Springer, New York, 1998), p. 116.
[36] P. Blaha, K. Schwarz, and J. Luitz, *Wien97, A Full Potential Linearized Augmented Plane Wave Package for Calculating Crystal Properties* (Technische Universität Wien, Austria, 1999).
[37] U. S. Whang, E. T. Arakawa, and T. A. Callcott, Phys. Rev. B **6**, 2109 (1972).
[38] W. Schülke, H. Nagasawa, S. Mourikis, and A. Kaprolat, Phys. Rev. B **40**, 12215 (1989).
[39] W. Schülke, H. Schulte-Schrepping, and J. R. Schmitz, Phys. Rev. B **47**, 12426 (1993).
[40] L. Hedin, Phys. Rev. **139**, A796 (1965).
[41] E.-N. Foo and J. J. Hopfield, Phys. Rev. **173**, 635 (1968).
[42] K. Sturm and L. E. Oliveira, Phys. Rev. B **30**, 4351 (1984).
[43] W. Schülke, H. Nagasawa, S. Mourikis, and P. Lanzki, Phys. Rev. B **33**, 6744 (1986).
[44] K. Sturm and L. E. Oliveira, Europhys. Lett. **9**, 257 (1989).